Expanded View Figures

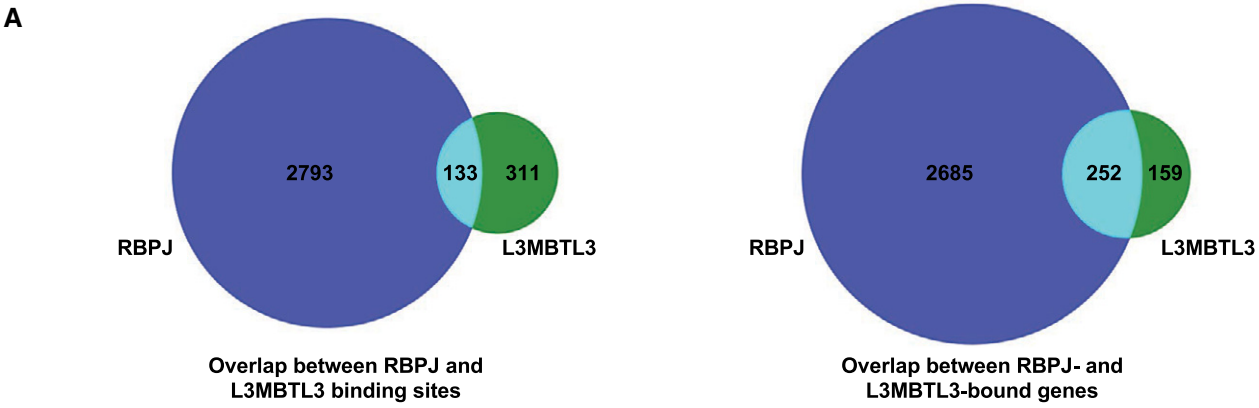

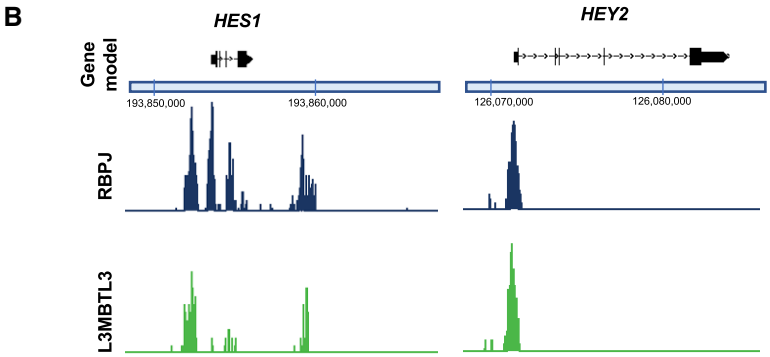

Figure EV1. RBPJ and L3MBTL3 co-localize genomewide in MDA-MB-231 cells.

A Venn diagram showing the genomewide co-localization of RBPJ and L3MBTL3.

B Snapshots showing the co-localization of RBPJ and L3MBTL3 at the *HES1* and *HEY2* loci.

◀ **Figure EV2. KDM1A interacts with L3MBTL3 and RBPJ.**

A L3MBTL3 and KDM1A interact in yeast two-hybrid assay. In this Y2H experiment, KDM1A is fused to the GAL4 DNA-binding (DB) domain and L3MBTL3 is fused to the GAL4 activation domain (AD). The DB-KDM1A and AD-L3MBTL3 fusion proteins interact with each other, leading to the activation of the *HIS3* reporter gene and allowing yeast cells to grow on selective media lacking histidine. The six Y2H controls have been previously described (Dreze *et al*, 2010). The experiment was independently replicated thrice.

B Endogenous RBPJ interacts with both endogenous KDM1A and endogenous L3MBTL3. IP of RBPJ in U87-MG or MDA-MB-231 cells using a RBPJ antibody followed by Western blot analyses using KDM1A, L3MBTL3, or RBPJ antibody. The experiment was independently replicated twice.

C L3MBTL3 interacts with KDM1A in IP experiments. *L3MBTL3* KO U87-MG cells were transfected with CRISPR/Cas9 sg-*L3MBTL3*-resistant plasmids encoding V5-L3MBTL3 WT or V5-L3MBTL3-Δ(1-64) mutant. IPs were performed using V5 antibody and the precipitates were analyzed via Western blotting using V5, KDM1A, or RBPJ antibody. The experiment was independently replicated twice.

D Endogenous KDM1A interacts with FLAG-HA-tagged RBPJ. IP of FLAG-HA-tagged RBPJ in U87-MG cells followed by Western blot analyses using RBPJ or KDM1A antibody. The experiment was independently replicated twice.

E Endogenous RBPJ interacts with FLAG-HA-tagged KDM1A. IP of FLAG-HA-tagged KDM1A in U87-MG cells followed by Western blotting analyses using FLAG or RBPJ antibody. The experiment was independently replicated twice.

F The SAM domain of L3MBTL3 is required for the L3MBTL3/KDM1A interaction. HEK293T cells were transfected with HA-tagged KDM1A and FLAG-tagged L3MBTL3 (WT or mutants, represented in Fig 2A). Upon IP with HA antibody, proteins were analyzed via Western blotting using HA or L3MBTL3 antibody. The experiment was independently replicated twice.

Data information: WB, Western blot; IP, immuno-precipitation; EV, empty vector control.
Source data are available online for this figure.

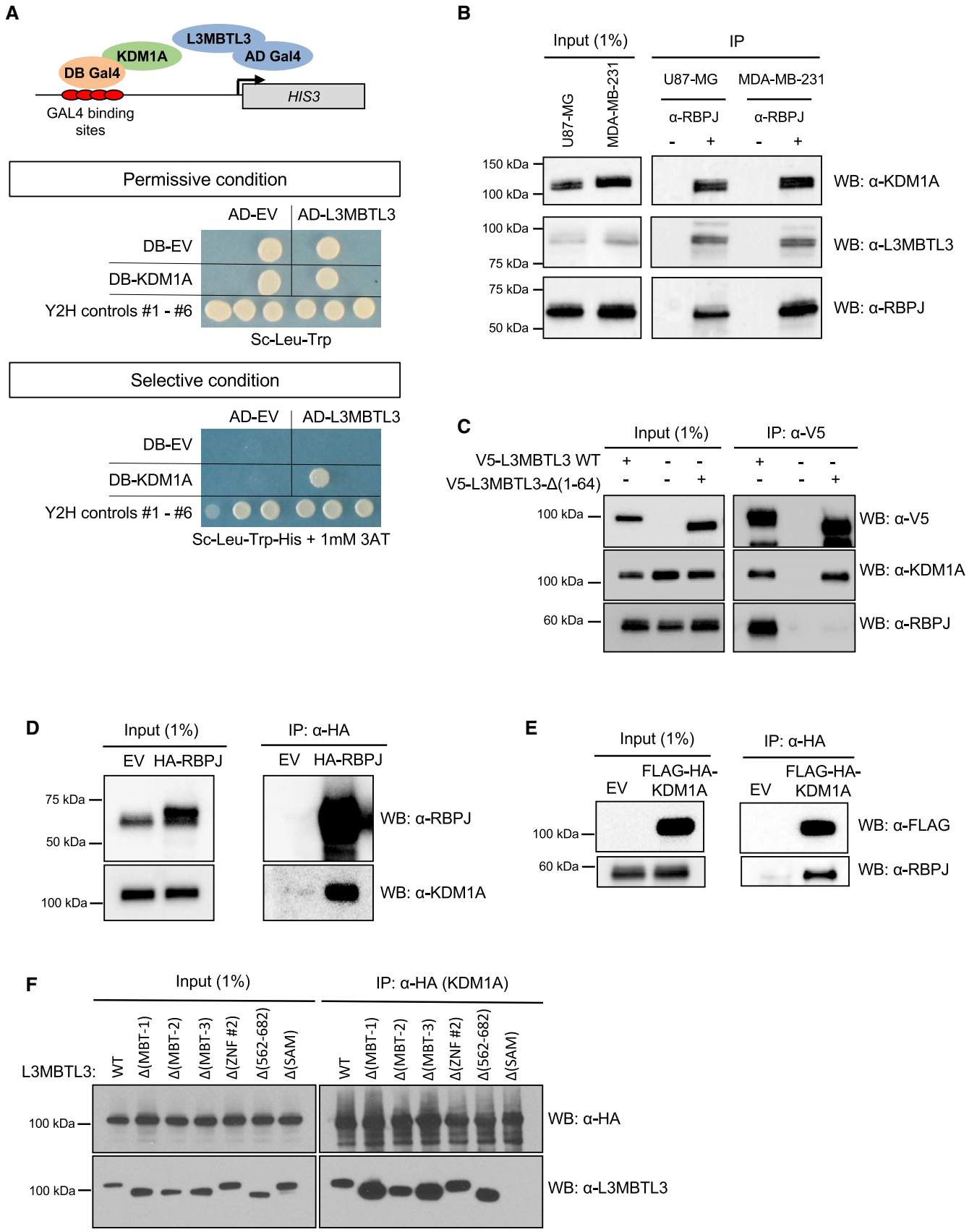
A
L3MBTL3
KDM1A
AD Gal4
DB Gal4
HIS3
GAL4 binding sites
Permissive condition
AD-EV
AD-L3MBTL3
DB-EV
DB-KDM1A
Y2H controls #1 - #6
Sc-Leu-Trp
Selective condition
AD-EV
AD-L3MBTL3
DB-EV
DB-KDM1A
Y2H controls #1 - #6
Sc-Leu-Trp-His + 1mM 3AT
B
Input (1%)
IP
U87-MG
MDA-MB-231
U87-MG
MDA-MB-231
α-RBPJ
α-RBPJ
- + - +
150 kDa
100 kDa
100 kDa
75 kDa
75 kDa
50 kDa
WB: α-KDM1A
WB: α-L3MBTL3
WB: α-RBPJ
C
Input (1%)
IP: α-V5
V5-L3MBTL3 WT + - - + - -
V5-L3MBTL3-Δ(1-64) - - + - - +
100 kDa
100 kDa
60 kDa
WB: α-V5
WB: α-KDM1A
WB: α-RBPJ
D
Input (1%)
IP: α-HA
EV HA-RBPJ
EV HA-RBPJ
75 kDa
50 kDa
100 kDa
WB: α-RBPJ
WB: α-KDM1A
E
Input (1%)
IP: α-HA
EV
FLAG-HA-KDM1A
EV
FLAG-HA-KDM1A
100 kDa
60 kDa
WB: α-FLAG
WB: α-RBPJ
F
Input (1%)
IP: α-HA (KDM1A)
L3MBTL3:
WT
Δ(MBT-1)
Δ(MBT-2)
Δ(MBT-3)
Δ(ZNF #2)
Δ(562-682)
Δ(SAM)
100 kDa
100 kDa
WB: α-HA
WB: α-L3MBTL3

Figure EV2.

A

```
Human L3MBTL3          11   QEFDVFSVMDWK-DGVGTLPGSDLKFRVNEFGALEVITDEN   50
Consensus              11   ~~~d~~~~LeWk-dgiatLpGS~lkFr~nEfg~levi~~~~   50
                            +.++.+++|||| ||||+|||||||||||||+||||+++.
Consensus             658   ~~~~~v~aLdWK~DGIaTLPGSnLrFRiNEFG~LEVItd~~   698
Drosophila dL(3)mbt   658   SMMQNLNMLKWRGQQPANLQNSTVRFELNEFNFLQINERCQ   698

Confidence score            348899999999 99999999999999999999999854
```

Identity: 0.20 - Similarity: 0.49 - Score: 130.7 - *P*-value: 6 E-19

B

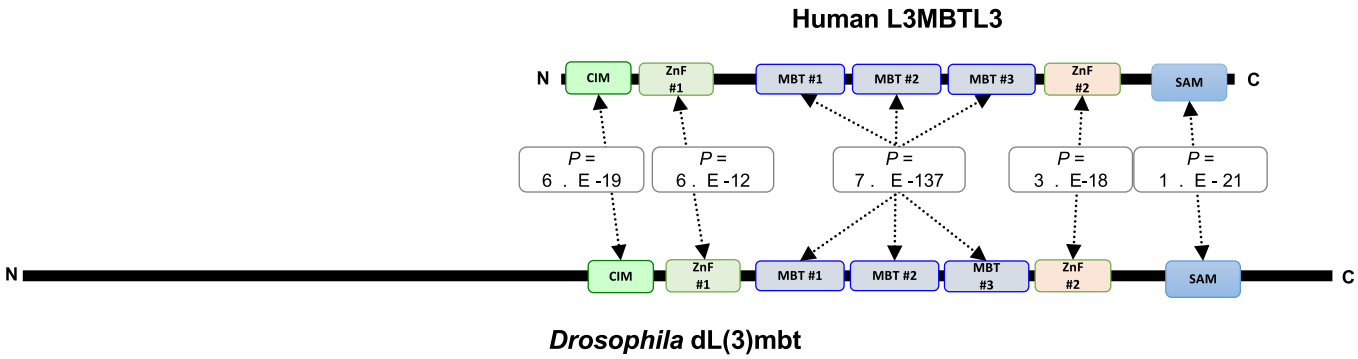

Figure EV3. The L3MBTL3-(1-64) domain is conserved in dL(3)mbt.

A Summary of the analysis of the amino acid sequences of human L3MBTL3 and *Drosophila* dL(3)mbt using a hidden Markov model (HMM) profile alignment approach (Soding, 2005). L3MBTL3-(11-50) and dL(3)mbt-(658-698) regions are conserved ($P = 6 \times 10^{-19}$). The consensus sequences identified in the HMM profile–profile alignment analysis are series of tildes, and amino acid letters that represent the calculated order of most frequent residues found at each position in the multiple sequence alignment analyses for L3MBTL3 or dL(3)mbt and their homologs across species. An "uppercase letter" refers to a residue having high conservation in the profile. A "lowercase letter" refers to a residue having significant conservation in the profile. A "~ symbol" refers to a position where no single residue stands out as being the most conserved. Between the alignments, the symbols indicate the overall value of aligning a pair of residues at a particular position: "." indicates a score between −0.5 and +0.5; "+" indicates a score between +0.5 and +1.5; "|" indicates a score > +1.5; "empty space" indicates a gap in the alignment.

B Schematic representation of the human L3MBTL3 and the *Drosophila* dL(3)mbt proteins. The analysis of the amino acid sequences using the HMM profile alignment approach generated highly confident alignments for seven conserved domains: the CSL interaction motif (CIM), the MBT domains #1, #2, and #3, the SAM domain, and the ZnF domains #1 and #2. *P* values are shown for each pair of conserved domains.

◀ **Figure EV4. Gain of *dL(3)mbt* suppresses *Notch*-induced hyperplasia in the *Drosophila* eye imaginal disk.**

Flies were grown at 25°C. Eye imaginal disks dissected from third-instar larvae of the indicated strains were labeled with EdU (red; to mark dividing cells) and subsequently stained with α-dNICD (green) and α-elav (blue; to mark differentiated cells) antibodies. *E1-Gal4* is an eye-specific *UAS* driver.

A–D Disks dissected from *E1-Gal4* control larvae present a normal morphology with a clear linear demarcation of EdU-positive dividing cells at the level of the morphogenetic furrow (red arrow in panel D), an indentation that demarcates the boundary between elav-positive developing photoreceptors located posteriorly and elav-negative undifferentiated cells located anteriorly.

E–H HA-dL(3)mbt overexpression alone has minimal effect on disk size or proliferation compared to *E1-Gal4* control.

I–L Ectopic expression of dNICD results in enlarged and distorted eye disks. Yellow arrows mark regions of high *UAS-dNICD* expression.

M–P Gain of *dL(3)mbt* significantly suppresses the dNICD-induced hyperplasia. Yellow arrows mark regions of high *UAS-dNICD* expression.

Q–T To assess the potential effects associated with *UAS* titration, the number of *UAS* constructs was normalized with *UAS-GFP* so that every genotype contained two *UAS* constructs. Disks were labeled with EdU (red) and counterstained with DAPI (blue). Note that the additional *UAS-GFP* transgenes do not affect the EdU staining pattern or overall disk morphology (compare panels A, E, I, and M to panels Q, R, S, and T, respectively), demonstrating that *UAS* titration is not responsible for the *UAS-HA-dL(3)mbt;UAS-NICD* phenotype.

Data information: At least 10 disks for each genotype were analyzed. Representative images are shown. Scale bars: 50 μm.

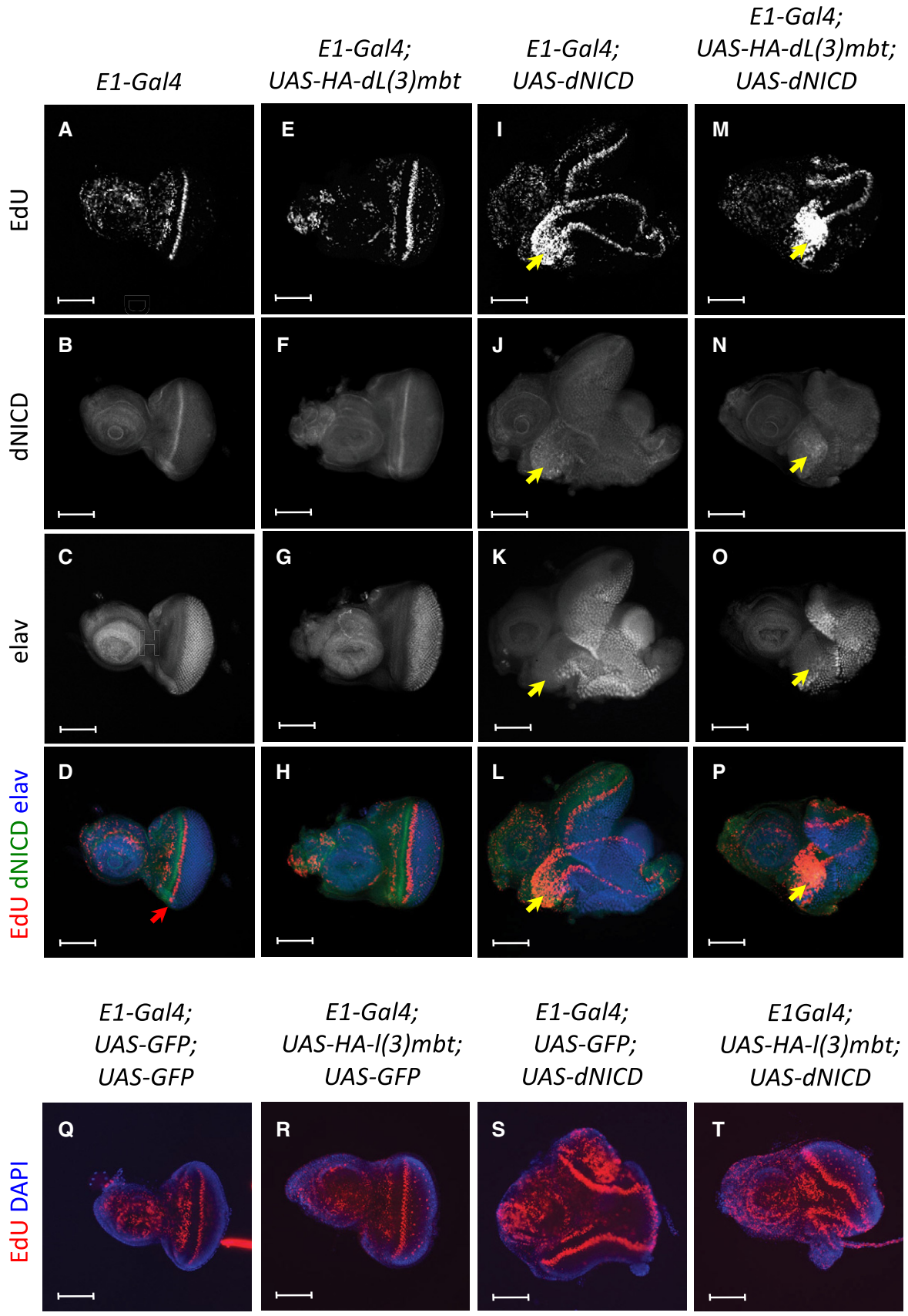

Figure EV4.

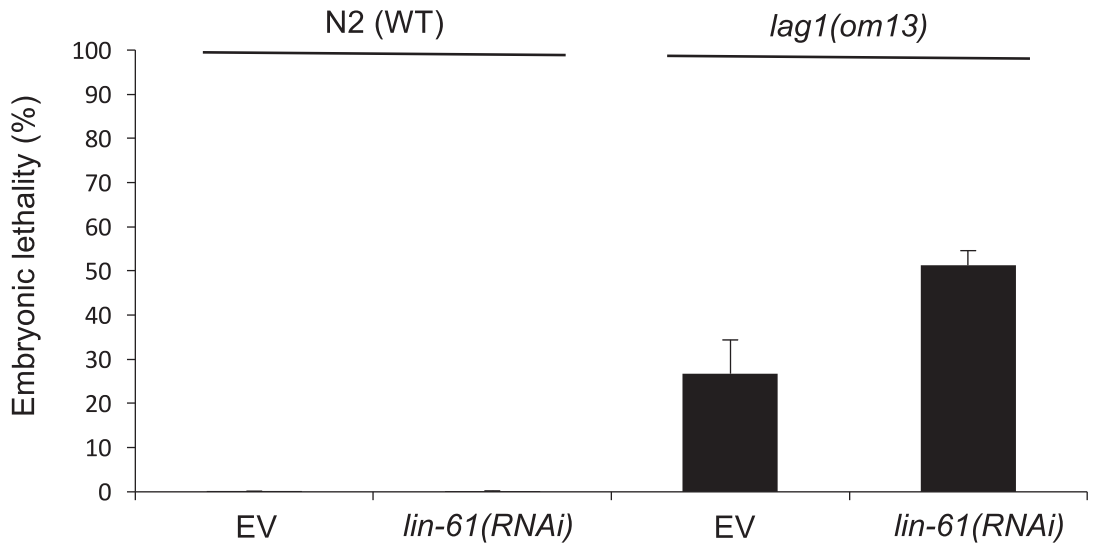

Figure EV5. Functional interaction between *lag-1/RBPJ* and *lin-61/L3MBTL3* during *Caenorhabditis elegans* embryonic development.
Proportion of dead embryos ($n \geq 700$) of N2 (N2 refers to the WT strain) and *lag-1(om13)* mutant animals fed with or without *lin-61(RNAi)* bacteria. The progeny of six to eight animals grown at 25°C was scored for embryonic lethality. Shown are means ± s.d. of duplicate experiments. EV, empty vector control.